

Regular magnetic fields in the dwarf irregular galaxy NGC 4449

K.T. Chyży¹, R. Beck², S. Kohle³, U. Klein³ and M. Urbanik¹

¹ Astronomical Observatory, Jagiellonian University, ul Orła 171, PL30-244 Kraków, Poland

² Max-Planck-Institut für Radioastronomie, Auf dem Hügel 69, D-53121 Bonn, Germany

³ Radioastronomisches Institut der Universität Bonn, Auf dem Hügel 71, D-53121 Bonn, Germany

Received date/ accepted date

Abstract. We present a high-resolution VLA study of the total power and polarized radio continuum emission at 8.46 and 4.86 GHz of the irregular galaxy NGC 4449, known for its weak rotation and non-systematic gas motions. We found strong galaxy-scale regular magnetic fields, which is surprising because of a lack of ordered rotation required for the dynamo action. The strength of the regular field reaches $8 \mu\text{G}$ and that of the total field $14 \mu\text{G}$, comparable to that of the total magnetic field strength in radio-bright spirals. The magnetic vectors in NGC 4449 form radial “fans” in the central region and fragments of a spiral pattern in the galaxy’s outskirts. These structures are associated with large regions of systematic Faraday rotation, implying genuine galaxy-scale magnetic fields rather than random ones compressed and stretched by gas flows. The observed pattern of polarization B-vectors is similar to dynamo-type fields in normal spirals. Nonstandard, fast dynamo concepts are required to explain the observed field strengths, though it is unknown what kind of magnetic field geometry can be produced in slowly and chaotically rotating objects. The so far neglected role of magnetic fields for the dynamics and star formation in dwarf irregulars also needs to be revised.

Key words: Galaxies:magnetic fields – Galaxies:irregular – Galaxies:individual:NGC 4449 – Radio continuum:galaxies – Polarization

1. Introduction

The generation of large-scale galactic magnetic fields from small-scale field perturbations caused by turbulence (as postulated by the dynamo concept) requires a preferred sense of twisting of turbulent gas motions, called the α -effect (Wielebinski & Krause 1993). In normal spiral galaxies it is determined by Coriolis forces caused by the disk rotation giving rise to strong dynamo action and to the observed spiral-like regular magnetic fields (Beck et

al. 1996b). To make the dynamo process work, either the differential rotational shear or the galaxy’s angular speed (in case of rigid rotation) must exceed certain threshold values (Ruzmaikin et al. 1988).

Dwarf irregulars are small, low-mass galaxies with a patchy distribution of star-forming regions. Though they exhibit a large variety of rotation curves (Hunter et al. 1998a) many of them show slow rotation with much less rotational shear than in normal spirals. Some dwarf irregulars show complex velocity fields with chaotic motions comparable in speed to the overall rotation. Even if the dynamo could still work in such conditions, the generation time scales of the magnetic fields estimated from classical dynamo theory would be very long and strong large-scale magnetic fields are not expected. Their observational detection would mean that the dynamical role of global magnetic fields in gas dynamics and star formation in irregular galaxies has to be reconsidered.

Signatures of a global magnetic field were already detected in the Large Magellanic Cloud (LMC, Klein et al. 1993). However, this galaxy still shows a significant degree of differential rotation (Luks & Rohlfs 1992) so that, like in normal spirals, the standard dynamo process could be at work. In this paper we present a sensitive radio polarization study of the dwarf irregular galaxy NGC 4449 which exhibits only weak signs of global rotation (cf. also Sabbadin et al. 1984, Hartmann et al. 1986). The radial velocities in NGC 4449 relative to the systemic one reach $\pm 20 - 30 \text{ km/s}$. However, the analysis of the high-resolution HI data cube (kindly supplied by Dr D. Hunter) does not show the classical picture of a global rotation. Instead, NGC 4449 shows velocity jumps and gradients along both the major and minor axis with centroids not coincident with the optical centre. They are intermixed with chaotic velocity variations with an amplitude of about $10 - 15 \text{ km/s}$. These very complex and chaotic kinematics, partly due to the interactions with DDO125 (Hunter et al. 1998b) and possibly also to a high star formation rate, make NGC 4449 an interesting target to investigate the magnetic field structure under conditions very difficult for

Send offprint requests to: K. Chyży (chris@oa.uj.edu.pl)

Correspondence to: chris@oa.uj.edu.pl

Table 1. Basic properties of NGC 4449

Type	IBm	
R.A. (1950)	12 ^h 25 ^m 44.8 ^s	LEDA database
Decl. (1950)	44°22′08″	LEDA database
R.A. (2000)	12 ^h 28 ^m 11.3 ^s	LEDA database
Decl. (2000)	44°05′30″	LEDA database
Opt. extent ^{*)}	5.8′ x 4.5′	LEDA database
Position angle	45°	LEDA database
Inclination	43°	Tully (1988)
Distance	3.7 Mpc	Bajaja et al. (1994)
	1′ corresponds to	1.08 kpc
Abs. B-magn.	−18.5	Schmidt & Boller (1992)
M_{tot}	$7 \cdot 10^{10} M_{\odot}$	Bajaja et al. (1994)
M_{HI}	$2.3 \cdot 10^9 M_{\odot}$	Bajaja et al. (1994)

*) isophotal diameter at 25^m/(□″)

the classical galactic dynamo. The basic parameters of NGC 4449 are summarized in Table 1.

A low-resolution detection of polarized emission (Klein et al. 1996) showed that the magnetic field in NGC 4449 is running across its bright star-forming body, very different from that in normal galaxies. In this work we present a total power and polarization study of this galaxy with a resolution and sensitivity several times better than that in the work of Klein et al. (1996). The use of two frequencies (8.46 and 4.86 GHz) enables us to determine the distribution of Faraday rotation over the disk of NGC 4449, allowing to discriminate between the galaxy-scale uniform fields and those passively stretched and compressed in the gas flows powered by huge star-forming regions.

2. Observations and data reduction

The maps of total power and linearly polarized radio emission of NGC 4449 at 8.46 GHz and 4.86 GHz were obtained using the Very Large Array (VLA) of the National Radio Astronomy Observatory (NRAO)¹. To attain highest sensitivity to smooth extended structures the most compact (D) configuration was used. The observations were carried out on 30 August and 1 – 2 September 1996 using 27 antennas at two independent IFs, each with a bandwidth of 50 MHz, separated by 50 MHz, with 11^h integration time on NGC 4449 at 6.2 cm and 16^h at 3.5 cm. The data were reduced using the standard AIPS software package. The flux density scale and the position angle of polarization was calibrated by observing the point source 3C 286. Instrumental polarization was corrected by observing 1216+487, which was also used for gain and phase calibration. The calibrated and edited visibility data were

¹ The National Radio Astronomy Observatory is a facility of the National Science Foundation operated under cooperative agreement by Associated Universities, Inc.

cleaned and self-calibrated (in phase only) using the AIPS package, yielding maps of Stokes parameters I, Q and U.

These IUQ data were combined with Effelsberg measurements using the program EFFMERC, a version of the SDE task IMERG (Cornwell et al. 1995) modified by P. Hoernes (see Beck & Hoernes 1996a). This program deconvolves both clean maps with their beams, and Fourier transforms them back into the UV plane. Then a combination of Effelsberg data for small spacings and VLA data for large spacings is performed with a linear interpolation in the overlap domain. The combined data are transformed back into the image plane with the synthesized VLA beam. To avoid ring-like distortions around strong unresolved sources, introduced by the combination technique, the bright unresolved sources were first subtracted from the maps and added again after the combination (see Beck et al. 1997). For our 8.46 GHz map we used the single dish data at 10.55 GHz from Klein et al. (1996), scaled to our frequency. We used mean spectral index of -0.7 ($S_{\nu} \propto \nu^{\alpha}$). For 4.86 GHz we performed separate observations with the 100-m Effelsberg radio telescope at 4.85 GHz.

The Q and U maps were combined to get maps of the linearly polarized emission (corrected for the positive zero level offset) and of the position angle of polarization E-vectors. The final maps have the synthesized beam of 12″ at 8.46 GHz and 19″ at 4.86 GHz. To obtain the map of Faraday rotation the data at both frequencies were convolved to a common beam of 19″.

3. Results

3.1. Total power and polarized emission at 8.46 GHz

The total power map of NGC 4449 at 8.46 GHz with apparent B-vectors of polarized intensity is shown in Fig. 1. As no correction for Faraday rotation was applied, the orientation of observed B-vectors may differ from the magnetic field directions by some 3° – 6° on average in the disk, the maximum difference reaching $\simeq 10^{\circ}$ in small regions of high Faraday rotation measures (see Sect. 3.3). The map shows details of the radio structure in the inner disk. The total power emission shows strong peaks at the position of bright star-forming regions. In addition to that diffuse radio emission away from the optically bright star-forming body has been detected as well. This radio envelope extends along the galaxy’s minor axis up to 2′ (corresponding to $\simeq 2.2$ kpc) from the main plane. The extent of the radio envelope at 8.46 GHz is larger than that of the faint diffuse H α emission (see Fig. 1). In the southern disk the radio emission has an extension towards a nebulous object at RA₂₀₀₀ = 12^h28^m06^s.7, Dec₂₀₀₀ = 44°03′39″ (probably a supernova remnant), forming a faint peak at its position.

The contour map of polarized brightness with apparent B-vectors proportional to the polarization degree is

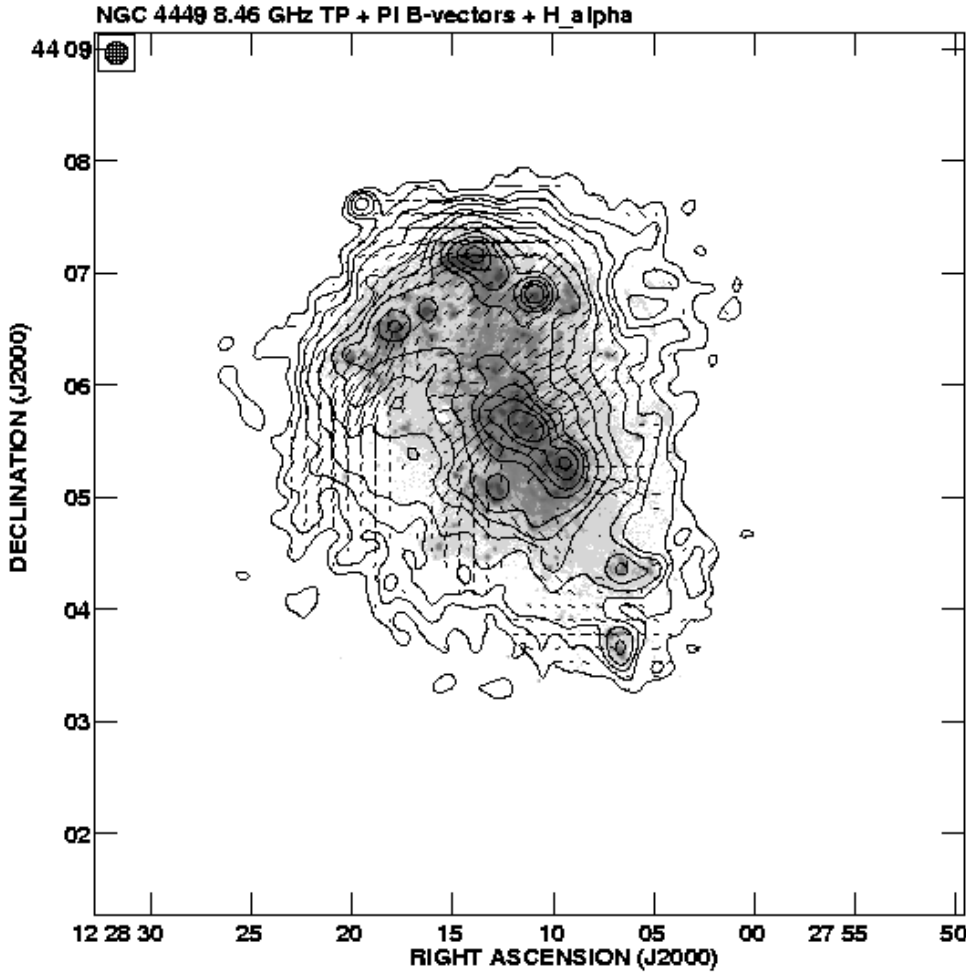


Fig. 1. The total power contour map of NGC 4449 at 8.46 GHz with observed B-vectors of polarized intensity (taken as perpendicular to E-vectors) superimposed onto the H α image of Bomans et al. (1997), digitally enhanced to show the low-brightness details of the ionized gas distribution. The resolution of the radio map is 12". The contour levels are (3, 5, 7, 10, 15, 20, 30, 60, 90, 140, 200) $\times 13 \mu\text{Jy/b.a.}$, the r.m.s. noise level of the total power map. Vectors of 10" correspond to 50 $\mu\text{Jy/b.a.}$

shown in Fig. 2. The extended radio emission is substantially polarized (locally up to 50%), with extended (≥ 1 kpc) domains of highly aligned B-vectors. The magnetic field structure in the inner disk looks unusual at first glance (Figs. 1 and 2). The projected magnetic vectors in NGC 4449 show two distinct kinds of structure. From the bright central star-forming region they are directed radially outwards, on each side forming a polarized “fan”. The B-vectors are parallel to the H α filaments discussed in detail by Sabbadin & Bianchini (1979) and by Bomans et al. (1997). In the galaxy’s outskirts, the magnetic vectors run along a polarized ridge encircling the galaxy on the northern, north-eastern and eastern side. Between this structure and the eastern “fan” an elongated unpolarized “valley” is due to a geometrical superposition of mutually perpendicular polarization directions in the “fan” and in the polarized ridge.

3.2. Total power and polarization at 4.86 GHz

Our maps at 4.86 GHz have a considerably worse resolution than those at 8.46 GHz, and the orientations of the B-vectors may be subject to stronger Faraday rota-

tion (on average about 10° but locally up to $\simeq 30^\circ$, see Fig. 5). However, due to a higher signal-to-noise ratio at 4.86 GHz the radio emission is traced much further out (Fig. 3). At this frequency we can trace the radio envelope in the sky plane out to $3/2$ (3.5 kpc) from the galaxy’s major axis. The nonthermal emission thus extends into the halo beyond one isophotal (at the level of $25^m/(\square'')$) major axis radius, which is a rare (though not exceptional) phenomenon among spiral galaxies (e.g. Hummel et al. 1991).

The map at 4.86 GHz again shows the polarized “fans”, however the eastern one is less conspicuous at this frequency than at 8.46 GHz, which suggests stronger Faraday depolarization in this region. The polarized ridge in the northwestern portion of the galaxy, already visible in Fig. 2, turns out to be part of a larger polarized ring surrounding the galaxy from the northeast through north, east and south down to the southwest, with a well-organized, coherent pattern of magnetic vectors (Fig. 4). Another weak fragment of the polarized ring is visible west of the centre. The ring coincides well with a similar feature visible in HI (Hunter, priv. comm., Fig. 4), with one of the brightest polarization peaks lying close to the densest neu-

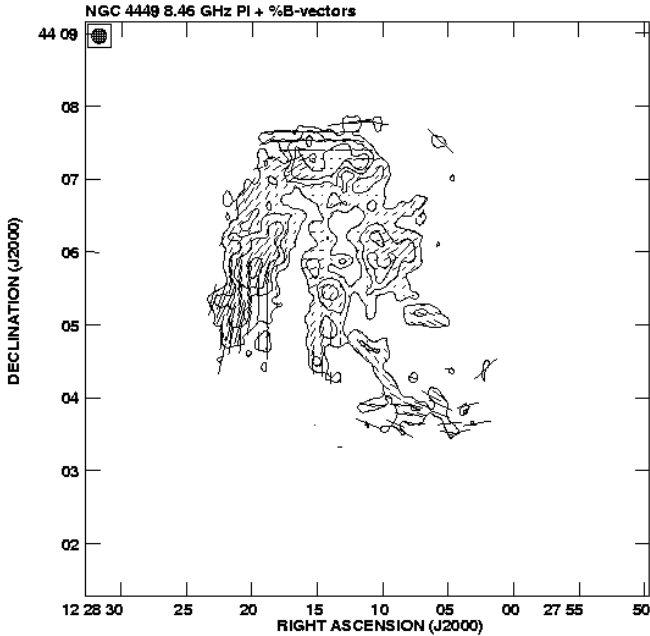


Fig. 2. The contours of polarized intensity of NGC 4449 at 8.46 GHz with superimposed B-vectors (perpendicular to the observed E-vectors) of the polarization degree. The contour levels are $(2, 4, 6, 9) \times 9 \mu\text{Jy/b.a.}$, the r.m.s. noise of the polarized intensity map. Vectors of $10''$ correspond to 20%

tral gas clump. Along the ring the polarization B-vectors are not exactly tangential to the azimuthal directions or to the HI shell. They deviate systematically from the azimuthal directions by some $20^\circ - 40^\circ$. A detailed discussion of the magnetic field directions is presented in Sect. 4.

Due to the higher sensitivity at 4.86 GHz our map shows very well the unpolarized “valley” not only at the interface of the eastern “fan” and the ridge but also a similar feature in the NW disk. In both cases they result from a geometrical superposition of magnetic field directions in the “fans” and in the polarized ring, seen almost perpendicular to each other when projected to the sky plane.

3.3. Faraday rotation

The distribution of Faraday rotation measures between 8.46 and 4.86 GHz is shown in Fig. 5. The northern and eastern parts of the polarized ring, as well as the “magnetic fan” east of the central star-forming complex show coherently positive Faraday rotation measures (RM) over areas with sizes of about $1.5'$, with a mean value of about $+50 \text{ rad/m}^2$. The values of RM are rising locally up to $+200 \text{ rad/m}^2$. The western “fan” and the southern part of the polarized ring are dominated by negative RMs, on average of about -50 rad/m^2 but also reaching -150 rad/m^2 locally. The errors in these regions vary from ± 10 to $\pm 20 \text{ rad/m}^2$ in regions of low RMs, exceeding $\pm 50 \text{ rad/m}^2$ in regions of high rotation measures. However, though in in-

dividual points the values of RM do not generally exceed the errors by more than $2 - 2.5\sigma$ r.m.s. errors, coherent areas of the same sign of RM extend over many beam sizes. The statistical significance of our determinations of RM is discussed in detail in Sect. 4.

4. Discussion

4.1. Distribution of thermal emission

In order to determine the equipartition magnetic field strength in selected regions of NGC 4449 we need to estimate the distribution of thermal emission in the galaxy. The spectral index computed between the maps of NGC 4449 at 8.46 GHz and 4.86 GHz changes from about -0.3 ($S_\nu \propto \nu^\alpha$) in strongly star-forming regions to -1.1 locally in the outer southern region. Somewhat smaller variations are found by Klein et al. (1996), probably because of the much lower resolution used by these authors. Although Klein et al. (1996) found variations of the nonthermal spectral index α_{nt} between -0.5 in the central star-forming region to -0.8 in the eastern part of the halo, for our purpose it was sufficient to assume α_{nt} constant over the whole galaxy. Possible uncertainties due to this assumption were included in the errors. To determine the nonthermal spectral index we compared the radial distribution of the thermal brightness S_{th} at 8.46 GHz and that in the $H\alpha$ line ($S_{H\alpha}$), convolved to the beam of $19''$. We found that they are identical for $\alpha_{nt} = -0.9$. This value differs only by about 1.5σ r.m.s. from the value obtained by Klein et al. (1996) from the radio spectrum, but agrees better with their estimate based on thermal flux obtained from the $H\alpha$ emission.

The distribution of thermal fraction f_{th} at 8.46 GHz in NGC 4449 (Fig. 6) shows clear peaks at the positions of bright star-forming complexes, f_{th} reaches 80% there. After subtraction of the thermal emission these regions are still considerably brighter than the diffuse emission from the surroundings by some 40%. Away from bright star-forming complexes the emission is largely nonthermal, the free-free emission amounts to not more than 10%.

As an additional test of our assumption of α_{nt} constant over the galaxy’s body we analyzed the point-to-point correlation between maps of the radio thermal flux at 8.46 GHz and that in the $H\alpha$ line convolved to $19''$. We checked that, using the Monte-Carlo simulations of two-dimensional arrays of points convolved to various beams, values in map points separated by 1.2 times the beam size are correlated only by some 10 – 12% and are for our purposes almost independent. Therefore we used points separated by 22.8 . In order to eliminate an artificial correlation caused by the radial decrease of all quantities, each map was divided by an axisymmetric model obtained by integrating the map in elliptical rings with the position angle and inclination taken from Tab. 1. A correlation slope significantly larger than 1 would mean that we have

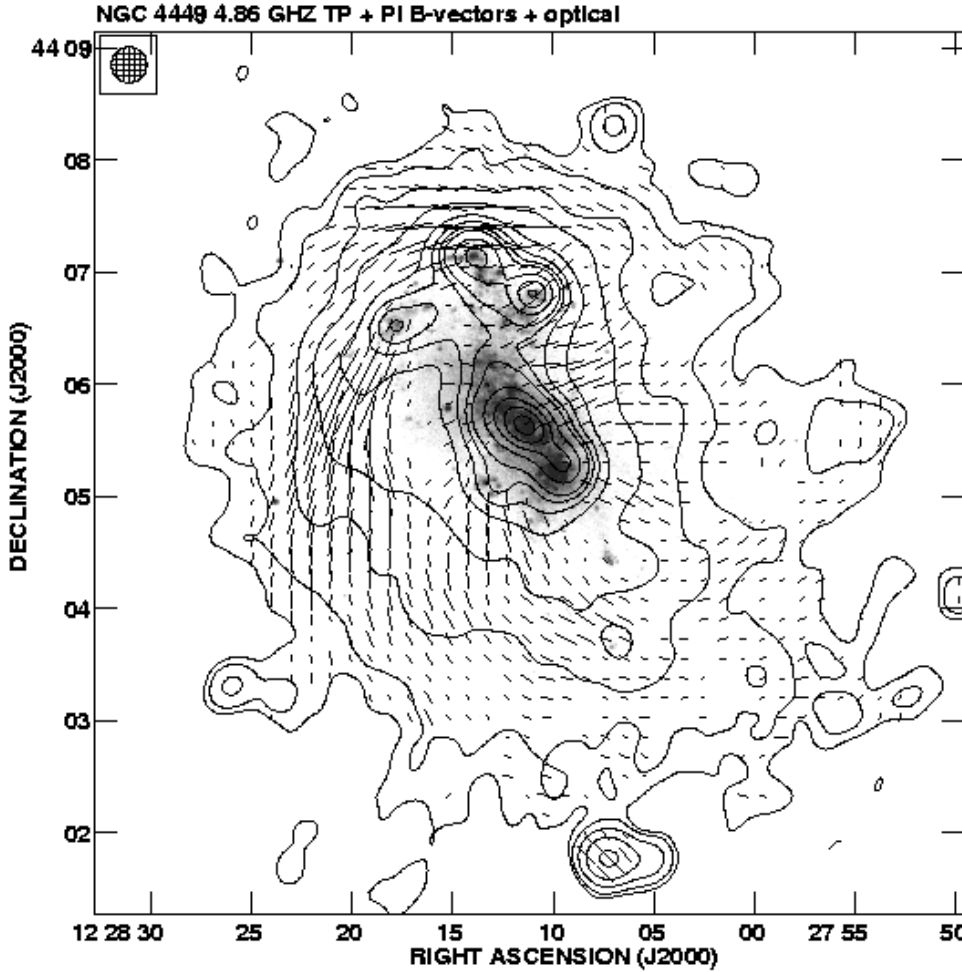


Fig. 3. The contour map of the total power of NGC 4449 at 4.86 GHz with B-vectors of the polarized intensity superimposed onto an optical image obtained by one of us (SK) at the Hoher List Observatory. The resolution is $19''$. The contour levels are (3, 5, 10, 20, 40, 60, 80, 100, 150, 200, 250, 300) $\times 26 \mu\text{Jy/b.a.}$, the r.m.s. noise in the total power map. Vectors of $10''$ correspond to $50 \mu\text{Jy/b.a.}$ No correction for Faraday rotation was applied (see Sect. 3.2)

overestimated the thermal radio emission in strongly star-forming regions while in fact they have much flatter non-thermal spectra. Using the orthogonal regression we obtained $S_{th} \propto S_{H\alpha}^{0.96 \pm 0.09}$, thus close to a linear relationship, though few regions deviate strongly from the best-fit line. This means that α_{nt} shows some place-to-place variations, but our assumption of $\alpha_{nt} = \text{constant}$ does not introduce large, systematic errors in determining the thermal fraction. A detailed multi-dimensional analysis of both radio emission components involving the $H\alpha$, CO, HI and X-ray data will be the subject of a separate study.

4.2. Magnetic field strengths

To determine the magnetic field strengths in NGC 4449 from the synchrotron emission we assumed the equipartition conditions between magnetic fields and cosmic rays to be valid everywhere in the galaxy. Furthermore we adopted a proton-to-electron ratio of energy densities of 100 and a lower energy cutoff of cosmic ray electrons of 300 MeV. We assumed a face-on thickness of the nonthermal disk of 2 kpc, resulting from a typical scale height of galactic radio disks of 1 kpc (Hummel et al. 1991), determined

Table 2. Magnetic fields in NGC 4449

Region	Position		total field μG	regular field μG
	RA ₂₀₀₀	Dec ₂₀₀₀		
Average for	NGC 4449		12 ± 4	4 ± 1
NW ridge	$12^h 28^m 14.5^s$	$44^\circ 07' 15''$	14 ± 4	7 ± 3
Eastern ridge	$12^h 28^m 20.5^s$	$44^\circ 05' 47''$	13 ± 4	8 ± 3
Western fan	$12^h 28^m 09.1^s$	$44^\circ 05' 51''$	14 ± 4	7 ± 2
Eastern fan	$12^h 28^m 14.2^s$	$44^\circ 05' 29''$	14 ± 5	6 ± 2

by the propagation range of cosmic ray electrons. With the inclination of NGC 4449 from Tab. 1 this implies a mean pathlength through the galaxy of 2.8 kpc. The errors of estimated magnetic field strengths include an uncertainty of these quantities of a factor two. The thermal fractions were taken from results described in Sect. 4.1.

Under these assumptions we determined the mean magnetic field strength for the whole galaxy and for selected regions; the results are summarized in Tab. 2. Regular magnetic fields derived from the polarized intensity

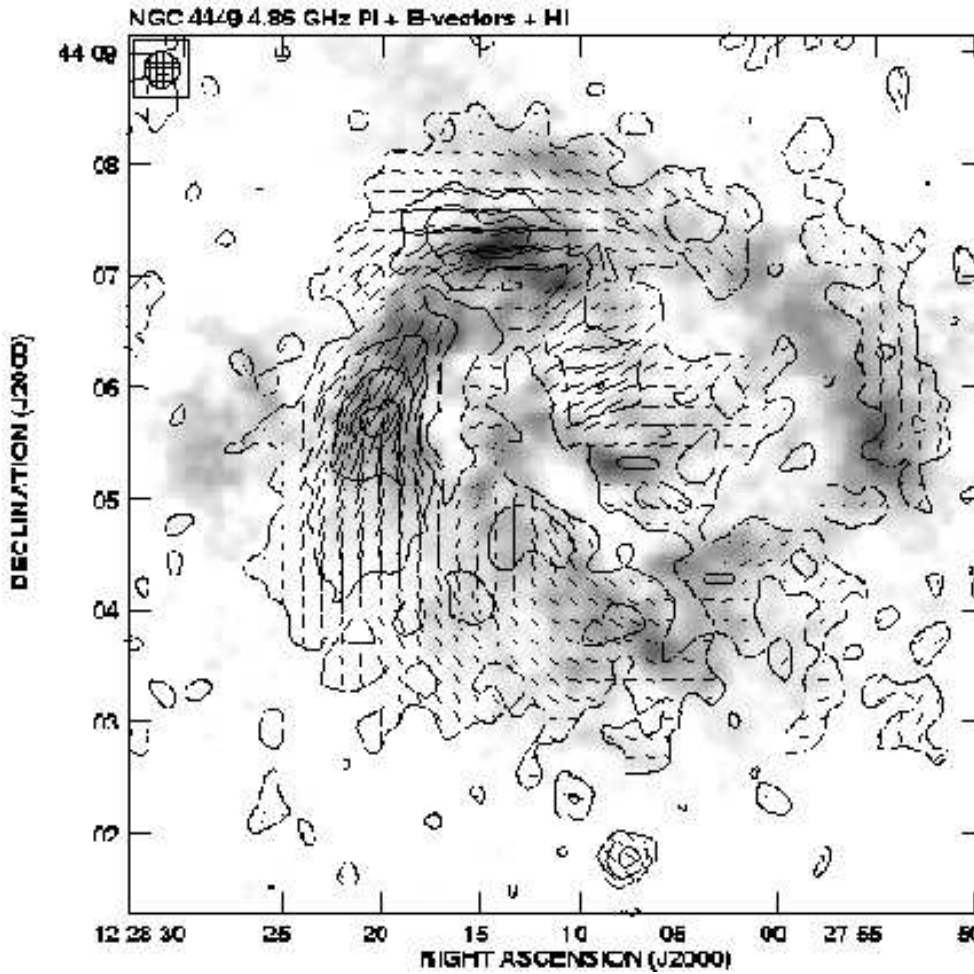


Fig. 4. Contours and B-vectors of the polarized intensity of NGC 4449 at 4.86 GHz with a resolution $19''$ superimposed onto a colour plot of the HI column density made from the data kindly supplied by Dr. D.A. Hunter from the Lovell Observatory. The contour levels of the polarized intensity are (3, 10, 20, 30, 35) $\times 5.4 \mu\text{Jy/b.a.}$, the r.m.s. noise level in the polarized intensity map

were found to reach locally up to $7 \pm 2 \mu\text{G}$ in the western magnetic “fan” and about $8 \pm 3 \mu\text{G}$ in the radio-bright part of the polarized ring. The total magnetic field in these regions, determined from the total power emission reaches $14 \pm 4 \mu\text{G}$, comparable to that in the radio-brightest spiral galaxies (Beck et al. 1996b). A slow rotation of NGC 4449 accompanied by chaotic gas motions apparently does not exclude the existence of strong, regular magnetic fields.

4.3. Magnetic field structure

4.3.1. Magnetic field coherence

The presence of polarized emission alone does not provide a definite proof for dynamo-generated, spatially coherent magnetic fields. Substantial polarization may be also produced by random fields, made anisotropic by squeezing or stretching, e.g. by stellar winds or large-scale shocks from multiple supernova events, however, frequent field reversals along the line of sight would completely cancel the Faraday rotation. Non-zero rotation measures imply the magnetic fields in the observed galaxy coherent over scales much larger than the telescope beam.

Although the values of RM in individual points of our Faraday rotation map (Fig. 5) do not exceed the errors by much, we note that they deviate coherently from zero, forming large domains of constant RM sign (both positive and negative). These regions with mean RM of $\simeq \pm 50 \text{ rad/m}^2$ are up to 20 times larger than the telescope beam area. A correction for the foreground rotation of -35 rad/m^2 was estimated from background sources present in our map and checked with the galactic RM map by Simard-Normandin & Kronberg (1980). At the galactic latitude of NGC 4449 of 72° the existence of foreground rotation structures changing sign over angular scales of $2' - 4'$ with an amplitude of 100 rad/m^2 , correlated with particular features in the galaxy’s polarized intensity, is unlikely. Thus, the observed Faraday effects almost certainly originate inside NGC 4449.

To check quantitatively the coherence of the non-zero Faraday rotation we computed values of RM and its error σ_{RM} in a grid of points separated by $22.8''$ (1.2 times the beam size). In case of a lack of systematic Faraday rotation such points would show only little correlation (see Sect. 4.1) and the variable defined as RM/σ_{RM} is expected to fluctuate randomly from point to point with a zero mean and unity variance. However, we found that

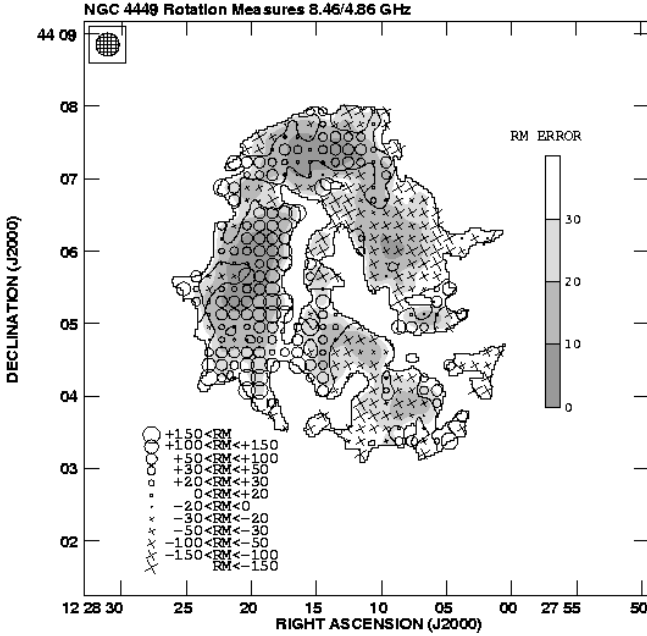


Fig. 5. The distribution of the Faraday rotation measures (RM) in the disk of NGC 4449, computed between 8.44 and 4.86 GHz. All data were convolved to a common beam of $19''$. Positive and negative values of RM are marked by circles and crosses, respectively. The symbol sizes indicate the absolute value of RM as indicated in the figure legend. The contour line divides the regions with positive and negative values of RM. The underlying greyscale plot shows the RM errors

its mean value deviates from zero in the eastern polarized ridge by more than $4.1\sigma_{mean}$ as well as in the western “fan” by more than $4.3\sigma_{mean}$, σ_{mean} being the r.m.s. error of mean RM in a given region. This implies that the probability of creating at random such large non-zero RM domains is less than 10^{-5} . In the eastern, weaker “fan”, the deviation amounts to only $1.6\sigma_{mean}$ (the probability of a random occurrence of non-zero RM of 10%), because of a worse signal-to-noise ratio. The results were found to be independent of the assumed foreground rotation. Thus we conclude that NGC 4449 contains genuine unidirectional fields, rather than stretched and compressed random magnetic field. The latter one would have different sky-projected components yielding a substantial polarization while the line-of-sight component would frequently change sign which would cancel any systematic Faraday rotation. We note that the growth of galaxy-scale coherent, unidirectional fields lies at the foundations of the dynamo process.

4.3.2. Magnetic field geometry

Fig. 7 a and b presents the distribution of magnetic field orientations in the azimuth- $\ln(R)$ frame (R being the radial distance from galaxy’s optical centre), in which the

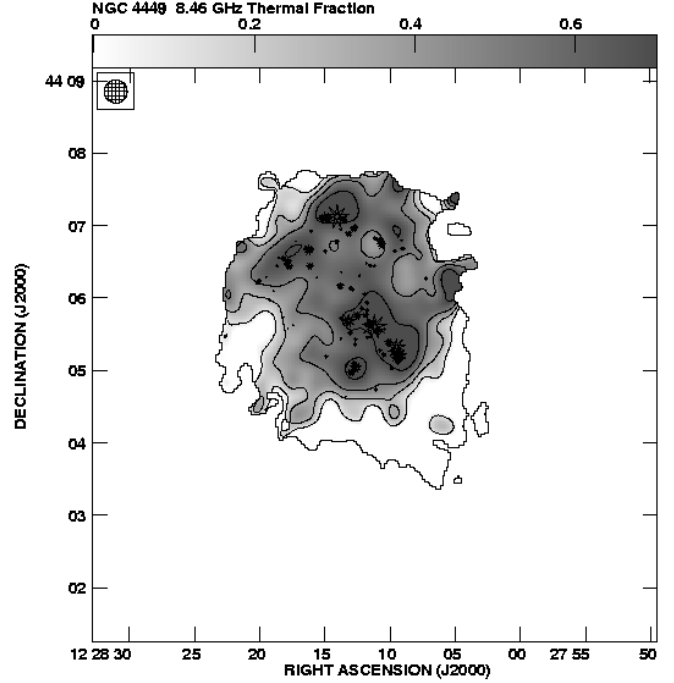


Fig. 6. The distribution of thermal fraction in NGC 4449 derived from the distribution of the spectral index between 8.46 GHz and 4.86 GHz. The data at both frequencies are convolved to a common beam of $19''$. The mean nonthermal spectral index of -0.9 has been adopted. The contour levels are: 0.1, 0.3, 0.5, 0.7. Symbols mark the positions of the brightest HII regions

logarithmic spiral appears as a set of straight lines inclined by the spiral’s pitch angle. At 8.46 GHz (little Faraday rotation) we clearly see a combination of the radial field in the inner region out to $\ln(R)$ of 0.5 – 0.6 and a more azimuthal one at larger radii. However, at this frequency the picture in the outer galaxy regions becomes rather noisy. A comparison of Figs. 7 a and b shows that Faraday rotation does not much change the global field picture in the inner region where the ionized gas density is highest and Faraday effects strongest. Thus, the 4.86 GHz data alone can be safely used in the galaxy outskirts.

Fig. 7b shows a very well ordered field in the polarized ring with the magnetic pitch angle ψ keeping a constant sign over most of azimuthal angles (except a low signal-to-noise region at azimuths of $0^\circ - 60^\circ$ and $\ln(R) \geq 1$). The value of ψ is $\simeq 40^\circ$ on average, with local variations. It resembles a somewhat distorted magnetic spiral with a substantial radial component. This, like in rapidly rotating spiral galaxies, may signify dynamo-type fields (Urbanik et al. 1997), while the random field pushed away from the galaxy and squeezed by an expanding gaseous shell would yield the observed B-vectors parallel to the shell. Nevertheless, the pitch angles show some place-to-place changes, possibly due to processes like local outflows or compressions. The strongest distortion of the spiral - the

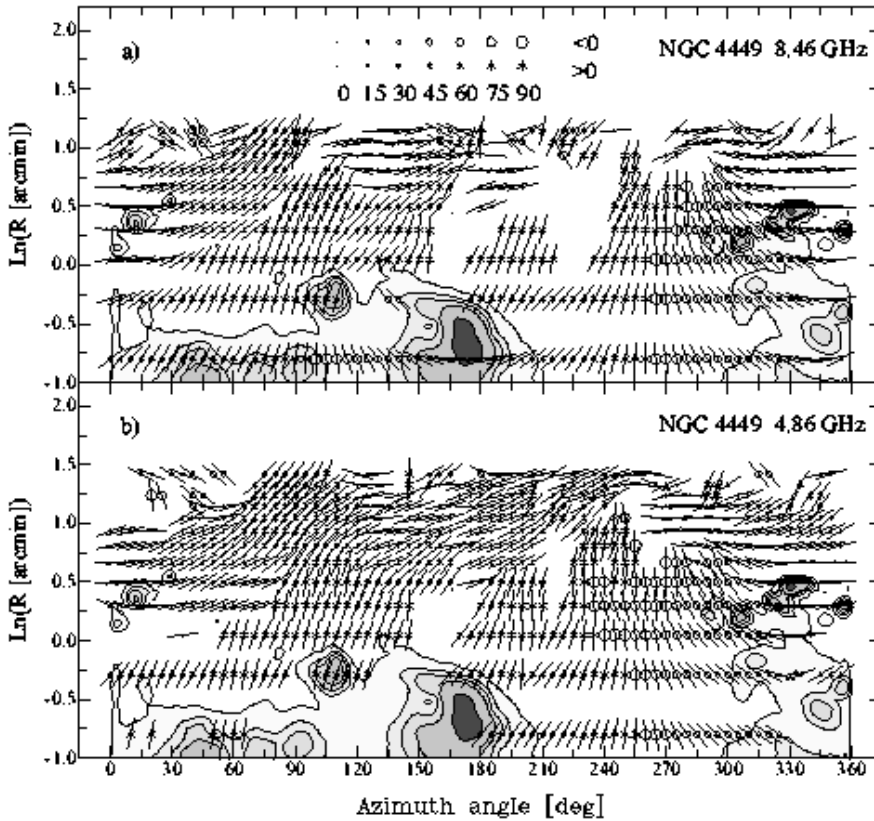


Fig. 7. The distribution of magnetic pitch angles in the disk of NGC 4449 at 8.46 GHz (a) and 4.86 GHz (b) as a function of azimuthal angle in the disk and $\ln(R)$, R being the galactocentric radius in arcmin. The data were corrected for the galaxy inclination taken from the LEDA database and refer to the galaxy’s main plane. The azimuthal angle runs counter-clockwise from the NE end of the major axis. The greyscale plot shows the distribution of the $H\alpha$ emission (Bomans et al. 1997) convolved to a Gaussian beam of $19''$. The size of symbols superimposed on the polarization B-vectors is proportional to the value of the magnetic pitch angle (see the legend in the Figure)

region of nearly pure toroidal magnetic field at azimuthal angles $\geq 270^\circ$, $\ln(R) \geq 0.5$ coincides with the densest HI clump and a region of star formation. The analysis of recent CO data (Kohle et al. in preparation) suggests strong gas compression possibly due to external interactions. We note also an opposite sign of Faraday rotation at both ends of the major axis, which is typical for axisymmetric magnetic fields.

The radial magnetic “fans” are structural elements not observed in spiral galaxies. They may be due to magnetic fields pulled out from the central star-forming region by gas outflows. Evidence for radial gas flows in NGC 4449 was indeed found by Martin (1998, 1999). However, in case of an initially random magnetic field (e.g. injected by supernovae) being stretched by gas flows, the “fans” would contain interspersed magnetic lines directed towards and outwards from the star-forming complex, yielding no significant Faraday rotation (see Sect. 4.3.1). Thus if the radial “fans” would result from the gaseous wind, a large-scale, coherent preexisting magnetic field would still be required, like one resulting from the dynamo process.

Alternatively, the observed magnetic field structure in NGC 4449 can be qualitatively explained by classical dynamo-generated fields. In addition to a toroidal field running around the disk, the classical dynamo process also generates a poloidal field with lines of force forming closed loop-like structures perpendicular to the disk plane and with diameters comparable to the galaxy radius (Donner

& Brandenburg 1990). They are due to a radial field component, B_r , turning into a vertical one, B_z , close to the centre and in the disk outskirts. The conservation of magnetic flux leads to B_z being always much stronger in the central region than in the outer disk. In large spiral galaxies the vertical segments of the poloidal field loops with the strongest B_z probably lie at heights $\geq 2 - 3$ kpc. This is too high to see the vertical magnetic field in synchrotron emission, as the latter has a vertical scale height of about 1 kpc (Hummel et al. 1991) due to a limited propagation range of cosmic ray electrons. As an exception NGC 4631 has a much larger scale height and dominating vertical fields in its inner regions (Hummel et al. 1991).

With its bright star-forming disk of about 4 kpc diameter NGC 4449 is several times smaller than normal spirals. If it had a classical poloidal dynamo-type magnetic field, its magnetic lines would make closed loop-like structures with a vertical size of about 1 – 1.5 kpc. The maximum B_z would occur at some hundreds of parsecs above the galaxy’s plane, well within the propagation range of radio-emitting electrons, making vertical fields visible in emission. The intense star formation in NGC 4449 and its low gravitational potential may give rise to galactic winds which may additionally enhance the generation of vertical magnetic fields (Brandenburg et al. 1993). With the inclination of NGC 4449 (Table 1) a strong poloidal field in the central part of NGC 4449, projected to the sky plane, may give rise to the observed radial magnetic “fans”. A detailed

MHD model of magnetic field evolution in NGC 4449 is a subject of a separate study (Otmianowska-Mazur et al., in prep.). We note also that superimposed on the global magnetic field, smaller-scale (< 0.5 kpc or $30''$ in our map) local phenomena (e.g. magnetized shells or giant magnetic loops caused by Parker instabilities, Klein et al. 1996) may be present, as well. They may explain e.g. local RM reversals, like that seen in the eastern “fan” at $\text{RA}_{2000} \simeq 12^{\text{h}}28^{\text{m}}12^{\text{s}}$, $\text{Dec}_{2000} \simeq 44^{\circ}04'30''$.

Although the dynamo process constitutes some possibility to explain the magnetic field structure in NGC 4449, the question arises how the dynamo mechanism can work in this galaxy. Despite some evidence for the dynamo action strong regular magnetic fields are hard to explain by classical dynamo models which, given the weak signs of rotation of NGC 4449, yield growth rates of the regular magnetic field at least an order of magnitude smaller than in rapidly rotating spirals (see e.g. Brandenburg & Urpin 1998). Estimates kindly provided by Dr Anvar Shukurov indicate that for the rotation speed and dimensions of NGC 4449 the classical, Coriolis force-driven α -effect is too weak for the onset of either $\alpha - \omega$ or α^2 dynamo (see Ruzmaikin et al. 1988 for definitions). Faster field amplification is predicted by a recent concept of the dynamo driven by magnetic buoyancy and sheared Parker instabilities (e.g. Moss et al. 1999). Crude estimates of its efficiency by A. Shukurov (priv. comm.) show that the α^2 dynamo process is easily excited throughout most of the galaxy’s body. However, what kind of structure is generated in such conditions remains still an open question and will be a subject of separate analytical and numerical studies.

Among other possibilities we can mention e.g. fast dynamos (Parker 1992), interrelations between small-scale velocity and magnetic field perturbations caused by specific instabilities (Brandenburg & Urpin 1998) or even magnetic field amplification without any α -effect at all (Blackman 1998). As in these concepts ordered rotation is still needed it is not known how they would work in the complex velocity field of NGC 4449. In summary, our work provides arguments in support of non-standard magnetic field generation mechanisms, though some elements of its structure may be due to gas outflow processes. Still a lot of theoretical work is needed to understand how a classical mixture of poloidal and toroidal fields, similar to that in rapidly rotating spirals can arise in a slowly and chaotically rotating object. Nevertheless, it seems that the existence of strong, dynamically important magnetic fields in dwarf irregulars cannot be ignored.

5. Summary and conclusions

We performed a total power and polarization study of the dwarf irregular galaxy NGC 4449 at 8.46 and 4.86 GHz using VLA in its D-configuration. The object rotates slowly and chaotically, thus no large-scale regular magnetic fields

were expected. To reach the maximum sensitivity to extended structures we combined our VLA data with the Effelsberg ones at 10.55 GHz and 4.85 GHz, respectively. Despite the slow and chaotic rotation of NGC 4449, unfavourable for dynamo-induced magnetic fields, we found it to possess strong regular, galaxy-scale fields.

The following results were obtained:

- NGC 4449 shows a large, partly polarized halo extending from its main plane up to 3.5 kpc, more than the isophotal major axis radius at $25^{\text{m}}/(\square'')$.
- The radio-brightest peaks coincide with strongly star-forming regions. These regions show increased thermal fractions (up to 80%), however the nonthermal emission is enhanced there as well.
- The galaxy possesses regular magnetic fields reaching locally $6 - 8 \mu\text{G}$, comparable to those in rapidly rotating spiral galaxies.
- NGC 4449 shows large domains of non-zero Faraday rotation measures indicating a genuine galaxy-scale regular magnetic field rather than random anisotropic ones with frequent reversals of their direction.
- The magnetic field structure consists of two basic elements: radial “fans” stretching away from the central star-forming complex and a magnetic ring at the radius of about 2.2 kpc. The magnetic field in the ring shows clear characteristics of a magnetic spiral with a substantial radial component signifying dynamo action.
- Both the radial “fans” and the polarized ring can still be explained in terms of a combination of sky-projected poloidal and toroidal dynamo-generated fields, taking into account the smaller size of NGC 4449 compared to normal massive spirals. Alternatively, magnetic “fans” could result from the gas outflow from the central star-forming complex. Even in this case a large-scale coherence of the magnetic field subject to stretching by outflows is required. Thus, some kind of dynamo action is needed, with a preference of non-standard (e.g. buoyancy-driven) dynamos. Whether and how this process can produce classical dynamo-like magnetic fields in a complex and chaotic velocity field of NGC 4449 remains yet unknown.

The detection of regular magnetic fields in spiral galaxies is important for understanding processes like turbulence, turbulent diffusion and the magnetic field generation in astrophysical plasmas; this is also of importance for plasma physics in general. It demonstrated that even in a highly turbulent medium large-scale regular fields can persist and grow quite efficiently. This has already boosted the development of dynamo theories applicable not only to a variety of astrophysical objects from planets to clusters of galaxies but also to laboratory plasmas. On the other hand, there was a widespread prejudice that all the mentioned concepts are restricted solely to rapidly rotating

plasma bodies. Against these expectations we show that strong regular fields can also arise in slowly and chaotically rotating systems. Their dynamical role in dwarf irregulars, especially in processes of star-formation triggered by magnetic instabilities, filament formation and confinement or even accelerating galactic winds via cosmic ray pressure exerted on MHD waves (Breitschwerdt et al. 1991), cannot be further neglected. NGC 4449 is the irregular galaxy with the best studied magnetic field so far. We believe that further progress needs more detailed models for such objects. Further detailed observations of the radio polarization of a larger number of irregulars with various morphological characteristics are also required.

Acknowledgements. The Authors wish to express their thanks to Dr Dominik Bomans from Astronomisches Institut der Ruhr-Universität Bochum for providing us with his H α map in a numerical format. We are grateful to numerous colleagues from the Max-Planck-Institut für Radioastronomie (MPIfR) in Bonn for their valuable discussions during this work. We want to express our profound gratitude to Dr Elly M. Berkhuijsen from MPIfR for her critical reading of the manuscript and precious suggestions concerning its improvement. M.U. and K.Ch. are indebted to Professor R. Wielebinski (MPIfR) for the invitations to stay at this institute where substantial parts of this work were done. One of us (K.Ch.) is indebted to Professor Miller Goss from NRAO for his invitation to Socorro and his assistance in some parts of data reduction. We are also grateful to colleagues from the Astronomical Observatory of the Jagiellonian University in Kraków for their comments. This work was supported by a grant from the Polish Research Committee (KBN), grant no. 962/P03/97/12. Large parts of computations were made using the HP715 workstation at the Astronomical Observatory in Kraków, partly sponsored by the ESO C&EE grant A-01-116 and on the Convex-SPP machine at the Academic Computer Centre "Cyfronet" in Kraków (grant no. KBN/C3840/UJ/011/1996 and KBN/SPP/UJ/011/1996).

References

- Bajaja E., Huchtmeier W.K., Klein U., 1994, A&A 285, 385
 Beck R., Hoernes P., 1996a, Nat 379, 47
 Beck R., Brandenburg A., Moss D., Shukurov A. Sokoloff D., 1996b, ARA&A 34, 155
 Beck R., Berkhuijsen E.M., Hoernes P., 1997, A&AS 129, 329
 Blackman E.G., 1998, ApJ 496, L17
 Bomans, D.J., Chu, Y.H., Hopp, U., 1997, AJ 113, 1678
 Brandenburg A., Donner K.J., Moss D., Shukurov A., Sokoloff D.D., Tuominen I., 1993, A&A 271, 36
 Brandenburg A., Urpin V., 1998, A&A 332, L41
 Breitschwerdt D., McKenzie J.F., Völk H.J., 1991, A&A 245, 79
 Cornwell T.J., Briggs D.S., Holdaway M.A., 1995, User Guide to SDE, NRAO, Socorro
 Donner K.J., Brandenburg A., 1990, A&A 240, 289
 Hartmann L.W., Geller M.J., Huchra J.P. 1986, AJ 92, 1278
 Hummel E., Beck R., Dahlem M., 1991, A&A 248, 23
 Hunter D.A., Elmegreen B.G., Baker A.L., 1998a, ApJ 493, 595
 Hunter D.A., Wilcots E.M., van Woerden H., Gallagher J. S., Kohle, S., 1998b, ApJ 495, L47
 Klein U., Haynes R. F., Wielebinski R., Meinert, D., 1993, A&A 271, 402
 Klein U., Hummel E., Bomans D. J., Hopp U., 1996, A&A 313, 396
 Luks Th., Rohlfs K., 1992, A&A 263, 41
 Martin C.L., 1998, ApJ 506, 222
 Martin C.L., 1999, ApJ 513, 156
 Moss D., Shukurov A., Sokoloff D., 1999, A&A 343, 120
 Parker E.N., 1992, ApJ 401, 137
 Ruzmaikin A.A., Shukurov A.M., Sokoloff D.D., 1988, Magnetic Fields of Galaxies. Astrophys. and Space Science Library, Vol. 133, Kluwer Academic Publishers
 Sabbadin F., Bianchini A., 1979, PASP 91, 280
 Sabbadin F., Ortolani S., Bianchini A., 1984, A&A 131, 1
 Schmidt K.-H., Boller T., 1992, Astron. Nachr. 313, 189
 Simard-Normandin, M. Kronberg P.P., 1980, ApJ 242, 74
 Tully R.B., 1988, Nearby Galaxies Catalog, Cambridge Univ. Press
 Urbanik M., Elstner D., Beck R., 1997, A&A 326, 465
 Wielebinski R., Krause F., 1993, A&AR 4, 449